Journal of Engineering Sciences
Vol 13, Issue 04, APRIL/2022
ISSN NO:0377-9254

URBAN CHANNEL LINK ANALYSIS AND VISUALIZATION USING RAY TRACING AND BEAMSTEERING

Atchi Vamsi Reddy[1], Jaya Shree Neelagiri[2], Mallikarjun Manas Mallareddi[3]

#1,#2,#3 Student, Department of EECE, GITAM (deemed to be University), Gandhi nagar Rushikonda Visakhapatnam 530045 Andhra Pradesh, INDIA

Abstract: Ray tracing propagation model uses ray tracing analysis to compute propagation paths and path losses. Path loss is considered from free space loss, reflection loss due to material, and antenna polarization loss. This method uses images but does not include effects from refraction, diffraction, scattering or transmission through buildings. Receiver site is defined in nLoS conditions which shows shadowing due to destruction. An imaginary LoS is plotted to show the blockage. Rays are plotted by adjusting propagation models to include single reflection paths. Propagation characteristics include received power, phase change, distance and angles of departure and arrival. Received power should be computed for each location using ray tracing propagation model with two reflection paths. This point-to-point analysis reveals some signal power reacting those locations. Beam steering technique is used to maximize received power for nLoS links. Get the angle-of-departure for the single reflection path and apply this angle to steer the antenna in the optimal direction to achieve higher received power. Ray tracing analysis can be used to predict signal strength for non-line-of-sight links where reflected propagation paths exist. Analysis with realistic materials can have a significant impact on the calculated path loss and received power. Analysis with higher number of reflections results in increased computation time but reveals additional areas of signal propagation. Usage of a directional antenna with beam steering can significantly increase the received power for receivers, even if they are in non-line-of-sight locations.

Keywords: Ray tracing propagation model, nLoS, predict signal strength.

1. Introduction

A key part of ray tracing methods is to determine the rays from a source location to a field point. In the simplest case, i.e., in free space, the procedure is trivial: there is only one ray present (the direct ray) which is a straight line from the source to the receive point. In an urban environment which is the most common scenario for using ray tracing, there may exist many rays from a source location to a field point; each ray may undergo different number of reflections, diffractions, or their combinations. To determine these rays is not a trivial task but has been a hot research area since the 1990's. It involves two aspects: fast ray-tracing algorithms and accurate field calculations. The ray tracing method has been widely used in radio propagation modelling and simulation. In this section we discuss the accuracy and recent development of propagation modelling related to ray tracing methods. Compared with measured results, ray tracing methods can provide satisfactory accuracy for path loss predictions. The ray tracing results are especially accurate when comparing the general tendency of simulated path loss (or the signal levels) with the measured results. Thus, an average process is usually used to filter out the sensitive local variations of the predicted results when the ray fields are added coherently. This is similar to the measurement process where mean received power is obtained by averaging the received signal along a line (straight or

circular) or over an area to filter out the small-scale fading. Ray tracing can also provide angle of arrival/departure, delay profile, and wideband results with good accuracy. The accurate modelling of the propagation environments plays an important role in the accuracy of the propagation modelling using ray tracing methods. For the urban scenarios, the building footprints and heights are usually known within limited accuracy. The effect of different building databases on ray tracing results is examined. It is reported that the building footprints can have one meter error without affecting the predicted path loss values. The effect of building footprints and heights on the ray tracing results are also reported. As more and more digital elevation data are available with better resolutions, it is getting more convenient to extract terrain features important for radio propagation modelling such as the mountain peaks and ridges. A simple method is used to extract 3D ridges from digital elevation data. The extracted ridges then serve as diffraction wedges in simulating the radio wave propagation. It is shown that 3D features of ridges, e.g., the orientation and elevation parameters, are necessary for accurate calculation of diffracted fields. These 3D features are commonly ignored in widely used propagation modelling methods such as the knife edge diffraction.

2. Literature survey

J. G. Marin and J. Hesselbarth [1] In this paper the Steering Efficiency Product (SEP) as a new figure of merit is proposed, which considers aperture efficiency (thus physical size and directivity), maximum beam-steering angle and maximum scan loss. S. Kim [2] The diffraction coefficients of a lossy dielectric are constructed routinely by employing the HRD technique.

W. Hong [3] For non- LOS communications, the single-directional beam needs to be steered either electronically or mechanically in order to find a reliable substitute link. Multi Beam Antennas hold great promise for enabling complex and secure wireless connections for high-speed data transmission in both base stations and user terminals of a 5G system. C. A. Balanis [4] Uniform arrays usually possess the largest directivity. However, super directive antennas possess directivities higher than those of a uniform array. Super directive arrays require very large currents with opposite phases between adjacent elements. Thus, the net total current and efficiency of each array are very small compared to the corresponding values of an individual element.

P. XingDong [5] Based on beamforming technology, the antenna array beam of a large MIMO device may be focused in a narrow range, potentially reducing interference. Massive MIMO systems can achieve high array gain, which reduces the constraints on linearity and accuracy of transmit power, increases RF power performance, and allows massive MIMO systems to be deployed. The active multibeam antenna system, which consists of tens or hundreds of antenna elements and transceivers, is the core technology of massive MIMO. L. Dussopt [6] Electronic beam switching is possible with transmit array antennas using switched antenna arrays as focal sources. Electronic beam-switching over a small angular sector is an appealing feature for making point-to-point links easier to deploy by self-aligning the antenna beams at each end of the grid. This reduces the risk of misalignment caused by strong winds.

J. G. Nicholls [7] The phased arrays can be easily scaled by simply increasing the array size and repositioning the feed antenna. Localized phase control for each array part, either by reflection phase tuning or transmission phase tuning, allows for full space, fixed-frequency pencil-beam steering. C. Shu [8] The high-gain reflector antenna's beam is extremely narrow; it must be steerable over certain angles with sufficient gain loss in order to create and sustain a

wireless connection, which is accomplished by mechanically rotating the reflector. Fast steering and high accuracy positioning are needed if the reflector has a relatively large aperture. M. U. Afzal [9] Reflectors are physically rotated along several axes to direct the beam, while antenna arrays use phase shifters to steer the beam electronically. Other aperture-type antennas and arrays of medium-to-high gains may also benefit from the beam steering approach using near-field phase transformation.

3. Proposed Method

The transmitter operates at a carrier frequency of 28 GHz with 5W power and uses the default isotropic antenna. A transmitter site is defined to model a small cell scenario in a dense urban environment. Ray tracing propagation model uses ray tracing analysis to compute propagation paths and path losses as show in figure 1. Path loss is considered from free space loss, reflection loss due to material, and antenna polarization loss. This method uses images but does not include effects from refraction, diffraction, scattering or transmission through buildings.

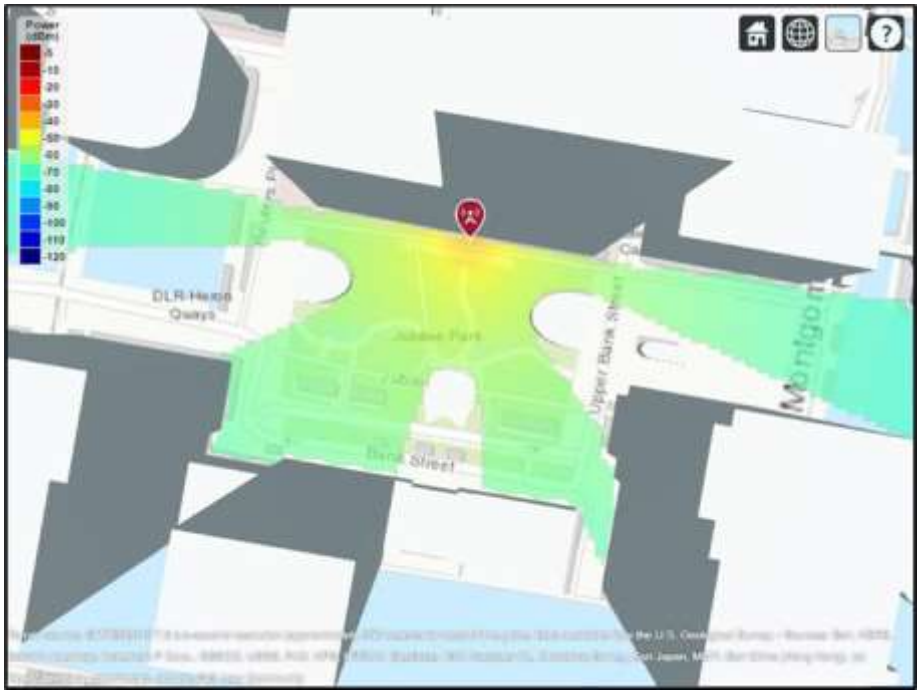

Figure 1. Area coverage of the transmitting antenna

Import and Visualize Buildings data

Imported an OpenStreetMap (.osm) file corresponding to Canary Wharf in London, UK. The file was downloaded from https://www.openstreetmap.org, which provides access to crowd-sourced map data all over the world. The data is licensed under the Open Data Commons Open Database License (ODbL). The buildings information contained within the OpenStreetMap file is imported and visualized in Site Viewer.

Figure 2. Imported 3D map

Define Transmitter Site: Defined a transmitter site to model a small cell scenario in a dense urban environment. The transmitter site represents a base station that is placed on a pole near a park with the purpose of servicing the park area. The transmitter operates at a carrier frequency of 28 GHz with 5W power and uses the default isotropic antenna.

Figure 3. Transmitting Antenna

View Coverage Map for Line-of-sight propagation: Created a ray tracing propagation model using the method of images. This propagation model uses ray tracing analysis to compute propagation paths and their corresponding path losses. Path loss is calculated from free-space loss, reflection loss due to material, and antenna polarization loss. The ray tracing analysis uses the method of images, which includes surface reflections but does not include effects from refraction, diffraction, scattering, or transmission through buildings. Figure 1 is the corresponding coverage map for a maximum range of 250 meters from the base station. The

coverage map shows received power for a receiver at each ground location but is not computed for building tops or sides.

Analyse a link in non-line of sight conditions: Receiver site is defined in nLoS conditions which shows shadowing due to destruction. An imaginary LoS is plotted to show the blockage as shown in the image. Rays are plotted by adjusting propagation models to include single reflection paths. Propagation characteristics include received power, phase change, distance and angles of departure and arrival.

Define receiver site in non-line-of-sight location: The coverage map for line-of-sight propagation shows shadowing due to obstructions. Defined a receiver site to model a mobile receiver in one such location. Plotted the line-of-sight path, which shows a blockage.

Figure 4. Non-line-of-sight receiver

Plot Propagation path using Ray Tracing: Adjusted the ray tracing propagation model to include single-reflection paths, and plot the rays. The result shows signal propagation along a single-reflection path. The plotted path may be selected to view the corresponding propagation characteristics, including received power, phase change, distance, and angles of departure and arrival.

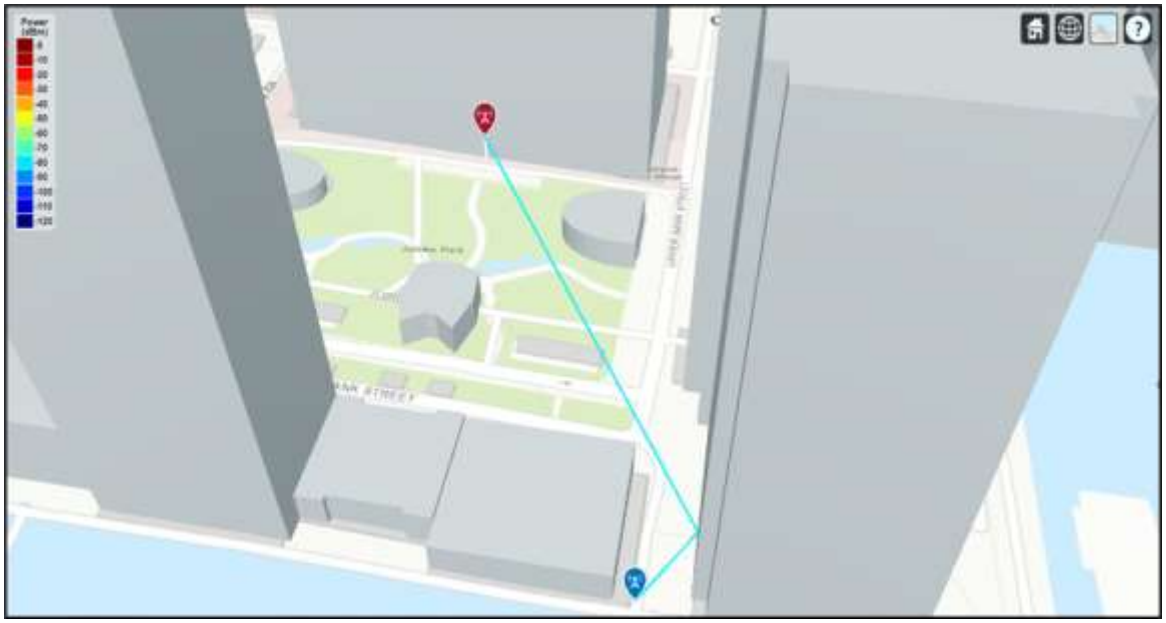

Figure 5. Using reflection to reach the receiver.

Analyze Signal Strength and Effect of Materials: Computed the received power using the propagation model which was previously configured to model perfect reflection. Assigned a more realistic material type and re-compute the received power. Updated the rays shown in figure 5. The use of realistic material reflection results in about 8 dB of power loss compared to perfect reflection.

Include Weather Loss: Added weather impairments to the propagation model and re-computed the received power, which results in another 1.5 dB of loss.

View Coverage map with Single Reflection paths: A coverage map is re-generated but included single-reflection paths and weather impairments. Loaded previously generated coverage results because otherwise the coverage analysis would take several minutes to complete. The resultant coverage map shows received power in the area around the non-line-of-site receiver analyzed above, but there are still some remaining regions where no signal appears to reach.

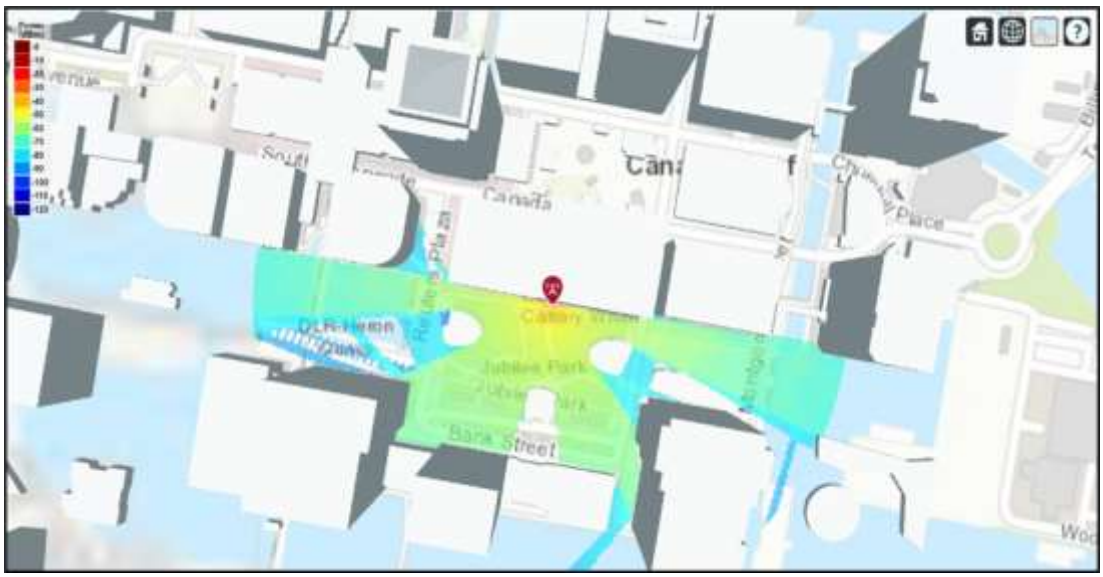

Figure 6. Transmission power mapping including reflection

Plot propagation paths including two reflections: Two reflection paths are enhanced to expand point to point analysis as shown in figure 7. The visualization shows two clusters of propagation paths and the total received power is enhanced by about 3 dB as compared to just considering single-reflection paths.

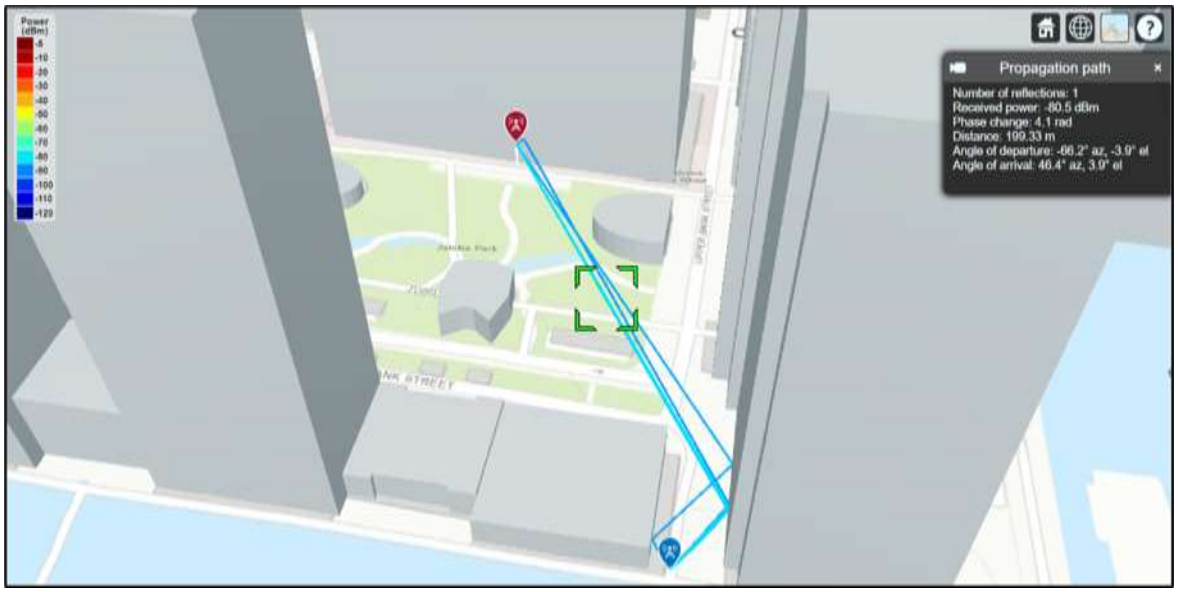

Figure 7. Propagation path including two reflections

Plot received power along the route with two-reflection analysis: The previous coverage map which included single-reflection paths showed some remaining holes in signal coverage. Defined several locations along a route that travels through two of the holes in the coverage map. The coordinates for each location were obtained by right-clicking on the map and selecting "Show location". Received power is computed for each location using ray tracing propagation model with two reflection paths. This point-to-point analysis revealed some signal power reaching those locations as shown in the figure 8.

Plotted the power at each location on the map, using the "streets-dark" base map to emphasize the data. The propagation Data object is used to plot the data, and this object could also be used to plot data imported from measurements files. The resultant plot shows low received power at the locations where there is neither line-of-sight nor single-reflection propagation.

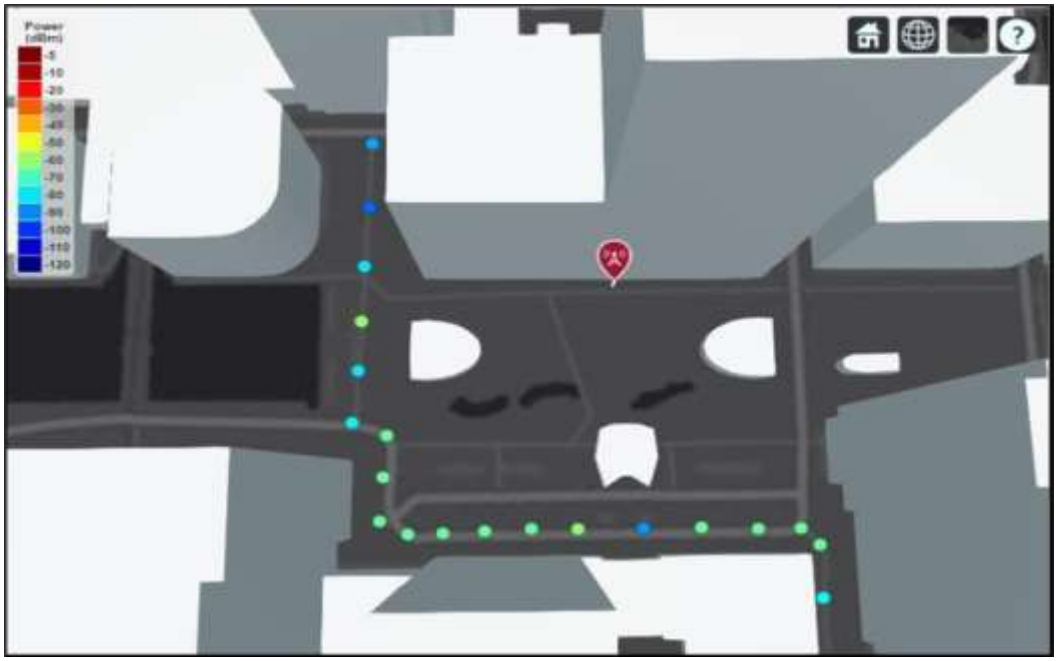

Figure 8. Possible receiver locations for a moving receiver along the route

Optimize a nLOS link using beam steering: Modern communication systems use beam steering technique to maximize received power for nLoS links. By creating an 8x8 uniform rectangular array from element pattern pointing towards the south, we analyse the radiation pattern. Get the angle-of-departure for the single-reflection path and apply this angle to steer the antenna in the optimal direction to achieve higher received power. The angle-of-departure azimuth is offset by the physical antenna angle azimuth to convert it to the steering vector azimuth defined in the phased array antenna's local coordinate system.

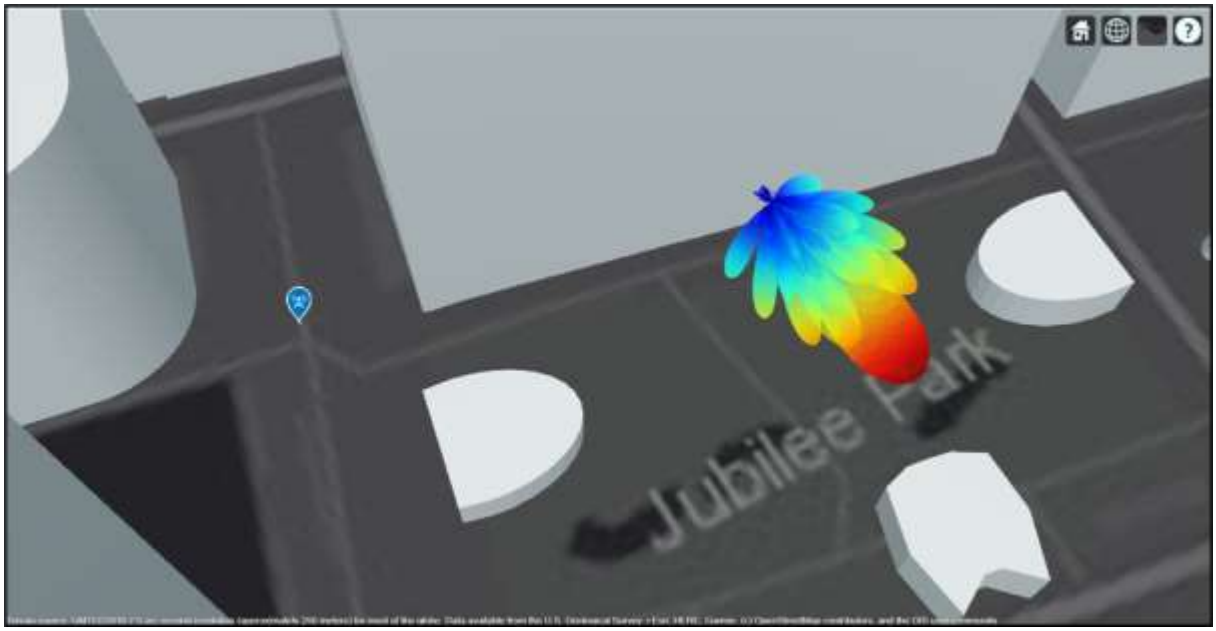

Figure 9. Beam of the transmitter

Radiation pattern is plotted to see how the antenna energy is directed along the propagation path. The new received power is enhanced by about 20 dB, corresponding to the peak gain of the antenna.

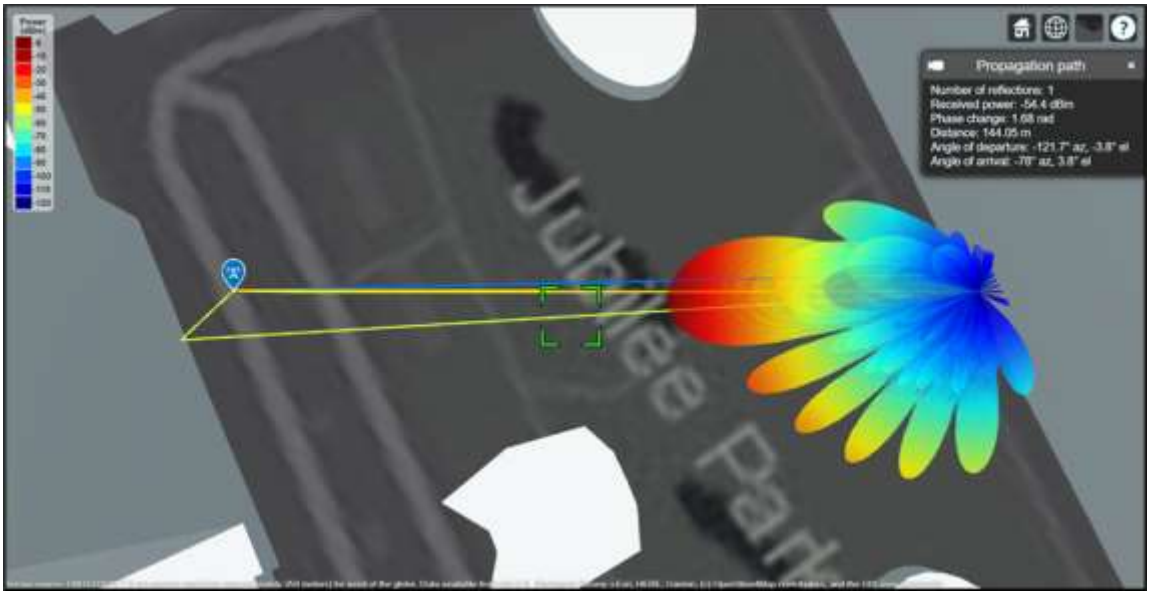

Figure 10. Beam Steering for a user location

4. Results and discussions

We performed the analysis at each receiver location which can be observed from figure 8. We obtained received power at all the mentioned locations in the code keeping the transmitter operating at 28GHz. We can observe the results from the below table.

Table 1. Recorded Observations at receiver locations along the route

S.No.	Latitude	Longitude	Received power(dBm)				
			Perfect Reflections	Concrete Materials	Weather loss	Two Reflection paths	Beam Steering
1	51.50216	-0.01769	-70.3925	-78.9451	-80.4625	-77.1419	-57.5028
2	51.502366	-0.017633	-69.5532	-77.9528	-79.3303	-76.1568	-56.5491
3	51.502571	-0.017575	-61.6803	-63.9542	-65.0583	-64.7346	-42.3836
4	51.502647	-0.017659	-61.3144	-64.2392	-65.2758	-64.7190	-42.7690
5	51.502674	-0.017905	-60.1080	-63.4913	-64.4738	-63.8574	-41.8833
6	51.502717	-0.018229	-60.1191	-63.0610	-63.9570	-63.4550	-40.9514
7	51.502753	-0.018561	--	--	--	-87.3111	--
8	51.502793	-0.018935	-58.8332	-61.3438	-62.2112	-61.0863	-39.2875
9	51.502825	-0.019198	-60.1700	-63.0949	-63.9948	-63.4836	-41.4917

10	51.502846	-0.019464	-60.6587	-63.4295	-64.3860	-63.7736	-42.4666
11	51.502865	-0.019703	-60.6090	-63.7885	-64.8246	-64.1125	-43.4923
12	51.502884	-0.019902	-61.8245	-64.4903	-65.5779	-65.1581	-44.8514
13	51.502953	-0.020048	-61.1118	-64.3783	-65.4930	-64.6513	-45.3237
14	51.503124	-0.019983	-61.9362	-64.0049	-64.9879	-64.6214	-45.4441
15	51.503288	-0.019917	-60.4748	-63.0145	-63.9227	-63.4975	-46.0720
16	51.503363	-0.020103	-70.9172	-79.0054	-80.6176	-76.6780	-58.5459
17	51.503570	-0.020013	-71.6921	-79.7690	-81.5317	-78.7225	-59.2900
18	51.503771	-0.019941	-58.6589	-61.0221	-61.8392	-60.9440	-54.5740
19	51.504001	-0.019864	--	--	--	-79.1917	--
20	51.504254	-0.019769	--	--	--	-93.1253	--
21	51.504535	-0.019681	--	--	--	-86.2582	--

- 8Db loss in the received power due to reflections of signals using concrete materials.
- We observed 1.5dB loss in the received power of signals due to weather loss.
- Total power is enhanced by 3dB due to transmitting the signal using two reflections.
- Locations where there is no power mentioned are locations where no propagation paths are found that meet required number of reflections. It can be observed from single reflection-based coverage map figure 6.

Conclusion: Ray tracing analysis can be used to predict signal strength for non-line-of-sight links where reflected propagation paths exist. Analysis with realistic materials can have a significant impact on the calculated path loss and received power. Analysis with higher number of reflections results in increased computation time but reveals additional areas of signal propagation. Usage of a directional antenna with beam steering can significantly increase the received power for receivers, even if they are in non-line-of-sight locations.

References

[1] J. G. Marin and J. Hesselbarth, "Figure of Merit for Beam-Steering Antennas," *2019 12th German Microwave Conference (GeMiC)*, Stuttgart, Germany, 2019, pp. 44-47.

[2] S. Kim, "Hidden Ray-Tracing on the Shadow Boundary of Penetrable Wedges," 2018 International Conference on Electromagnetics in Advanced Applications (ICEAA), Cartagena des Indias, 2018, pp. 146-147.

[3] W. Hong *et al.*, "Multibeam Antenna Technologies for 5G Wireless Communications," in *IEEE Transactions on Antennas and Propagation*, vol. 65, no. 12, pp. 6231-6249, Dec. 2017.

[4] C. A. Balanis, *Antenna theory: analysis and design,* New York, USA, Wiley, 2005, pp. 7, 283-333.

[5] P. Xingdong, H. Wei, Y. Tianyang, and L. Linsheng, "Design and implementation of an active multibeam antenna system with 64 RF channels and 256 antenna elements for massive MIMO application in 5G wireless communications," *China Communications,* vol. 11, no. 11, pp. 16-23, Nov. 2014.

[6] L. Dussopt, A. Moknache, T. Potelon, and R. Sauleau, "Switched-beam E-band transmitarray antenna for point-to-point communications," *11th Europ. Conf. Antennas Propag. (EUCAP),* Paris, 2017, pp. 3119-3122.

[7] J. G. Nicholls, and S.V. Hum, "Full-Space Electronic Beam-Steering Transmit array With Integrated Leaky-Wave Feed," *IEEE Trans. Antennas Propag.,* vol. 64, no. 8, pp. 3410-3422, 2016.

[8] C. Shu, S. Hu, Y. Yao, and X. Chen, "High-gain reflector antenna with beam steering for terahertz wireless communications," *10th UK-Europe-China Workshop on Millimeter Waves and TerahertzTechnologies (UCMMT),* Liverpool, 2017.

[9] M. U. Afzal, and K. P. Esselle, "Steering the beam of medium-to-high gain antennas using near-field phase transformation," *IEEE Trans. Antennas Propag,* vol. 65, no. 4, pp. 1680-1690, 2017.